Geodesy and Geodynamics xxx (xxxx) xxx

Contents lists available at ScienceDirect

Geodesy and Geodynamics

journal homepage: http://www.keaipublishing.com/geog

Review of the SBAS InSAR Time-series algorithms, applications, and challenges

Shaowei Li, Wenbin Xu*, [1], Zhiwei Li

School of Geosciences and Info-Physics, Central South University, Changsha 410083, China

ARTICLE INFO

Article history:
Received 26 May 2021
Accepted 8 September 2021
Available online xxx

Keywords:
InSAR
Small baseline subset
Time-series InSAR
Deformation

ABSTRACT

In the past 30 years, the small baseline subset (SBAS) InSAR time-series technique has emerged as an essential tool for measuring slow surface displacement and estimating geophysical parameters. Because of its ability to monitor large-scale deformation with millimeter accuracy, the SBAS method has been widely used in various geodetic fields, such as ground subsidence, landslides, and seismic activity. The obtained long-term time-series cumulative deformation is vital for studying the deformation mechanism. This article reviews the algorithms, applications, and challenges of the SBAS method. First, we recall the fundamental principle and analyze the shortcomings of the traditional SBAS algorithm, which provides a basic framework for the following improved time series methods. Second, we classify the current improved SBAS techniques from different perspectives: solving the ill-posed equation, increasing the density of high-coherence points, improving the accuracy of monitoring deformation and measuring the multi-dimensional deformation. Third, we summarize the application of the SBAS method in monitoring ground subsidence, permafrost degradation, glacier movement, volcanic activity, landslides, and seismic activity. Finally, we discuss the difficulties faced by the SBAS method and explore its future development direction.

1. Introduction

Geological disasters pose a massive threat to human life and property safety and have become a significant factor affecting the sustainable development of the regional economy and society. Most geological disasters are caused by surface deformation. Therefore, it is critical for disaster prevention and mitigation to monitor surface displacement and analyze the inner mechanism of geological disasters. Traditional geodetic surveying includes leveling, GPS, and other field measurement technologies. They have high measurement accuracy but require considerable workforce and material resources, and it is challenging to monitor large-area ground deformation. InSAR is a new type of earth observation technology with all-day, all-weather working ability and strong signal penetration ability, which provides a choice for surveying large-area ground displacement.

In 1969, Roger and Ingalls took the lead in using the InSAR technique to successfully extract the elevation information of the surface of Venus and the moon [1]. The original purpose of applying InSAR was to simultaneously obtain surface elevation by the phase difference of two SAR images [2]. As the SAR imaging theory matured, Gabriel et al. [3] proposed differential radar interferometry (D-InSAR), which realized the separation of ground elevation and deformation signals. Since then, D-InSAR has been widely used to measure deformations caused by natural phenomena such as earthquakes, volcanoes, and glaciers [4–6], as well as monitoring ground displacement caused by human activities, such as mining and reclamation [7,8]). However, the D-InSAR technique is often disturbed by atmospheric effects and spatio-temporal decorrelation noise [9,10]. The first error term is due to the unstable atmospheric conditions at two imaging moments, which causes a phase

* Corresponding author.
E-mail address: wenbin.xu@csu.edu.cn (W. Xu).

Peer review under responsibility of Institute of Seismology, China Earthquake Administration.

[1] Present/permanent address. School of Geosciences and Info-Physics, Central South University Changsha 410083, China.

Production and Hosting by Elsevier on behalf of KeAi

https://doi.org/10.1016/j.geog.2021.09.007

delay in the propagation of the radar signal. The other is generated when the scattering characteristics of the object change at different imaging moments. Much research has been devoted to the time-series method to avoid the influence of the error terms. For example, Sandwell et al. [11] assumed that the atmospheric phase is a random process in time, and the displacement exhibits a linear trend, and proposed the stacking InSAR algorithm. Ferretti et al. [12,13] found that when the amplitude deviation of a pixel is within a specific range, the phase stability of the pixel is better. These pixels were named permanent scatterers (PSs). When retrieving the time-series cumulative phase of these PSs from the single master stack interferograms, this method is referred to as permanent scatterer interferometry (PSI). Unlike PSI, Usai et al. [14] constructed a series of interferograms characterized by small spatio-temporal baselines, as shown in Fig. 1(b). They retrieved time-series cumulative deformation using the least-squares method. Compared with PSI, it is easier to avoid the influence of spatio-temporal decorrelation on the resulting solution. However, when multiple baseline subsets are formed, rank deficit problems occur during the least-squares solution process. Berardino et al. [15] introduced the singular value decomposition (SVD) algorithm in the deformation calculation process to solve rank deficit problems and developed it into the classic SBAS method.

Compared to D-InSAR, there are two apparent features [16] in the SBAS method. First, it requires many SAR images in the same area at different times. Second, it only extracts signals from points that feature stable scattering. In contrast, D-InSAR obtains deformation information at all points in the entire image. The above characteristics promote the SBAS method to achieve higher accuracy than D-InSAR. The SBAS method has become a reliable method for monitoring slow ground displacement [17] and has been widely used. It can be derived from the number of citations in Google Scholar that this method is becoming increasingly popular, as shown in Fig. 2.

The wide application and continuous development of the SBAS method may mainly benefit from the following two reasons. 1) Advancement of SAR satellite imaging techniques and data-processing capabilities. The SAR satellites were launched from the early low-resolution and medium-resolution SAR satellites such as ERS-1/2, ENVISAT, ALOS-1, and RADARSAT-1, to a new generation of high-resolution satellites such as TerraSAR-X, TanDEM-X, and Cosmo-SkyMed. The data sources used in the SBAS method is shown in Fig. 3. The new generation of SAR satellites is characterized by multi-polarization, multi-mode, multi-channel, high temporal and spatial resolution, and multi-satellite coordinated observation [19]. These further provide a basis for the theoretical research and application of the SBAS method. 2) The demand for projects to monitor ground deformation in a large area has stimulated the continuous development of time-series InSAR based on the SBAS method. The measurement capability and high precision of the SBAS method are convenient for further exploring the correlation between different factors and deformation phenomena to learn about the internal mechanism of the deformation process.

The SBAS method, as a representative time-series InSAR technique, has derived a variety of improved versions to solve different problems. Because of its excellent ability to survey ground displacement, this technique is suitable for different application scenarios such as subsidence, glacial movement [20], and mine deformation [21]. This article analyzes different SBAS methods and their research status in different fields to gain more systematic understanding. The core chapters of this article are arranged as follows. Section 2 outlines the principle and analyzes the limitations of the traditional SBAS method. Sections 3 and 4, present several improved SBAS methods and applications in different deformation scenarios. Finally, we discuss the challenges faced by the SBAS method, as well as the future development trends in the last two sections.

2. Classic SBAS method

2.1. Principle

The original $N+1$ SAR images covering a specific area generate M unwrapping interferograms by assuming that the spatio-temporal baseline is within a particular range. The points where the average phase coherence is more than a certain threshold are considered to be high-coherence points. The unwrapping phase of a high-coherence point (x, r) of the i-th unwrapping interferogram (corresponding to two moments t_1 and t_2) is expressed as follows:

$$\Delta\varphi_i(x,r) = \varphi_{t_2}(x,r) - \varphi_{t_1}(x,r) \approx \frac{4\pi}{\lambda}\left(\mathrm{d}(t_2,x,r) - \mathrm{d}(t_1,x,r)\right) + \Delta\varphi^i_{\mathrm{top}} + \Delta\varphi^i_{\mathrm{noise}} \tag{1}$$

where $\mathrm{d}(t_2,x,r)$ and $\mathrm{d}(t_1,x,r)$ represent the cumulative displacement of the radar line of sight (LOS) at t_1 and t_2 relative to the starting time, $\Delta\varphi^i_{\mathrm{top}}$ is the elevation residual phase caused by the DEM's inaccuracy; the noise phase such as the atmospheric phase screen and unwrapping error is usually expressed as $\Delta\varphi^i_{\mathrm{noise}}$. After removing the residual elevation phase, the phase is solved to solve the velocity term. The parameters to be solved are as follows:

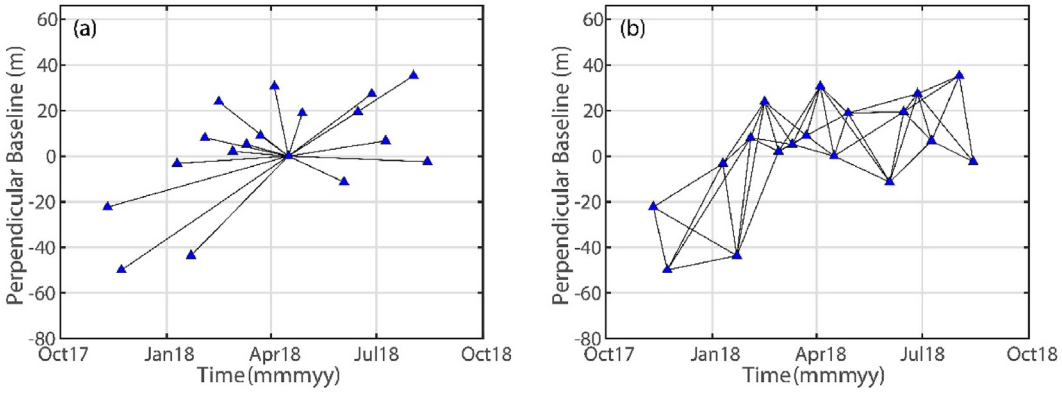

Fig. 1. Example baseline plot for (a) the PSI and (b) SBAS method.

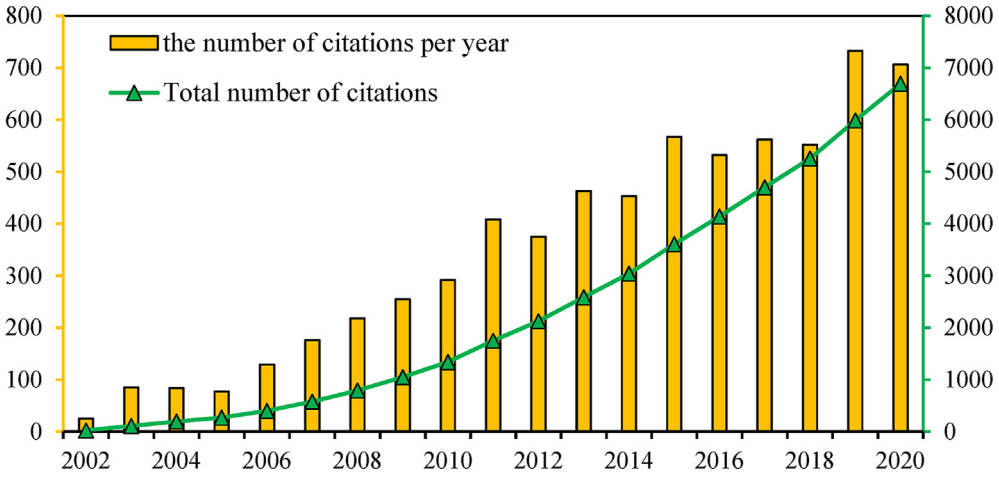

Fig. 2. Number of citations on the classic SBAS method (the data comes from Google Scholar [18]).

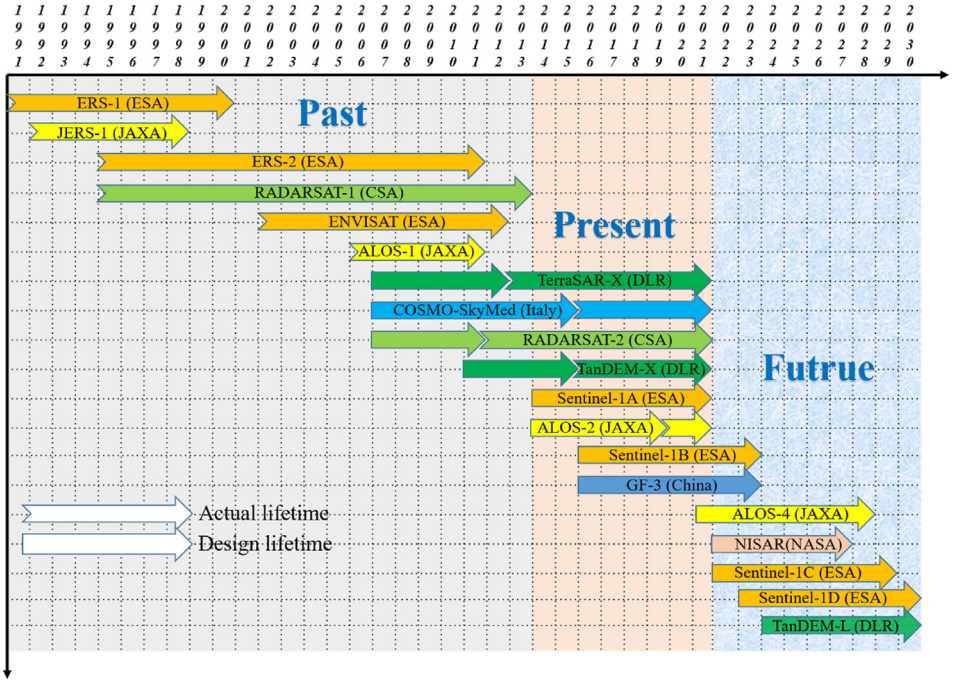

Fig. 3. SAR satellites are used as data sources for the SBAS method at different stages.

$$v^{\mathrm{T}} = \left[v_1 = \frac{\phi_1 - \phi_0}{t_1 - t_0}, \ldots, v_N = \frac{\phi_N - \phi_{N-1}}{t_N - t_{N-1}} \right] \tag{2}$$

The phase of the i-th unwrapping interferogram can be written as,

$$\sum_{t_{1,i}+1}^{t_2,i} (t_k - t_{k-1}) V_k = \Delta\varphi_i \tag{3}$$

The phases of all interferograms are expressed in the above form. The combined expressions are represented in the error equation as

$$\mathbf{A}V = \Delta\varphi \tag{4}$$

where A is a matrix with dimensions of $M \times N$. If a single interferogram subset is formed, the least-squares method can be used to solve the deformation rate. When two or more interferogram subsets are created, the singular value decomposition (SVD) method with minimum norm conditions needs to be introduced to obtain the deformation rate.

2.2. Limitations

The classic SBAS method mainly faces two deficiencies in introducing the above principles and practical applications. First, when the solution is existent, unique, and stable, the equation system (4) is considered to be well-posed. Otherwise, it is deemed ill-posed when any one of the conditions is not satisfied [22]. In general, the following two reasons may cause ill-posed problems:

First, when multiple subsets of interferograms are formed, the coefficient matrix of Equation (4) is the deficit. The classic SBAS method solves the rank deficiency problem using SVD. However, because the SVD algorithm sets the incremental phase delay among different baseline subsets to zero, this may lead to inaccurate calculations. Another reason is that when a specific SAR image and most other SAR images form interferograms, it can easily cause an approximately linear correlation of the coefficient matrix in Equation (4). Finally, it may face problems such as insufficient selection of stable points and difficulty in describing multi-dimensional deformation phenomena in practical applications.

3. Improved SBAS methods

The classic SBAS method inevitably has problems such as model errors and sparse stable points selected in a specific area, as mentioned in the previous section. A variety of improved SBAS methods have been developed to adapt the SBAS method to different application scenarios. The main SBAS method is shown in Fig. 4. These methods are classified and introduced from several different aspects: solving the ill-posed equation, increasing the density of high-coherence points, improving the accuracy of monitoring deformation, measuring the multi-dimensional deformation.

3.1. Solving the ill-posed equation

It is easy to encounter rank deficit problems and ill-conditioned problems when constructing the error equation, as described in Section 2.2. To solve the ill-conditioned equation, Lauknes et al. [23] introduced a regularization constraint. Moreover, different researchers have provided different solutions for the problem of rank deficiency in Equation (4). These methods are mainly divided into two categories: 1) Schmidt and Weener et al. [21,24] introduced temporal smoothing constraint conditions in the error equation by assuming equal acceleration of adjacent periods. They also discussed the method's reliability and found that this method can suppress the influence of atmospheric noise to a certain extent. 2) López-Quiroz and Doin et al. [25,26] considered that the deformation conforms to a relatively fixed-function mode as a temporal constraint condition and adjusts the degree of constraint by changing the constraint factor's value. This method is referred to as NSBAS Technology and is adopted by the LiCSBAS software developed by Yu Morishita et al. [27]. In addition, Usai and Liu et al. [28,29] added the minimum norm benchmark equation to solve the rank deficit problem and developed the constrained SBAS method (CSBAS). Therefore, we should choose the most appropriate method to solve different types of ill-posed problems in the data processing process.

3.2. Increasing the density of high-coherence points

The SBAS method is an opportunistic deformation measurement, that is, it only measures the deformation over high coherence points (HPs). However, the HP density is usually low in vegetated, forested, and low-reflectivity areas. In contrast, they are generally abundant in buildings and exposed rocks. To improve the monitoring ability of the classic SBAS method, it is crucial to increase the density of the HPs. The main options are as follows.

3.2.1. Full-resolution SBAS

The classic SBAS method was initially designed to monitor deformations occurring in a relatively large spatial area. One situation is that the traditional SBAS method may lead to sparse coverage of coherent points owing to its multi-look process. Therefore, it is not suitable for analyzing the local deformations that may be affected. To increase the density of the selected points, Lanari et al. [30] proposed a full-resolution SBAS method in 2004. The core idea of this method is as follows: First, we use the classic SBAS method on the multi-look differential interferograms to obtain the atmospheric phase screen, residual DEM error, and large-area surface deformation, which have the characteristics of low-frequency signals. This part of the low-frequency signal was removed from raw full-resolution differential interferograms. We then selected HPs on the residual full-resolution differential phase. The high-frequency linear and nonlinear deformations of the HPs were calculated using the maximum time coherence factor and SVD algorithm. The sum of the above three deformation signals is the actual ground deformation. The implementation process of this method is illustrated in Fig. 5. The full-resolution SBAS algorithm was tested relative to the Campania area (Italy) and validated using geodetic measurements since it was proposed. The results show that this method can achieve better accuracy.

Chandrakanta et al. [31] developed a constrained network propagation (C-NetP) scheme to improve the density of stable points selected by the full-resolution SBAS method in regions with low coherence, and successfully obtained the surface deformation of Rome, Italy. The research conclusions show that the proposed C-NetP method significantly increases the density of HPs by approximately 250%. In general, the full-resolution SBAS method increases the density of HPs and is suitable for detecting the deformation of small targets, such as bridges, buildings, and railways.

3.2.2. Intermittent SBAS (ISBAS)

In addition, the points selected by the classical SBAS method are relatively sparse in the vegetation coverage area owing to the temporal decorrelation effect. Therefore, Sowter et al. [32] changed the point selection method to make the SBAS method suitable for rural and natural surfaces in 2013. The ISBAS method considers each interferogram separately, selecting and unwrapping pixels

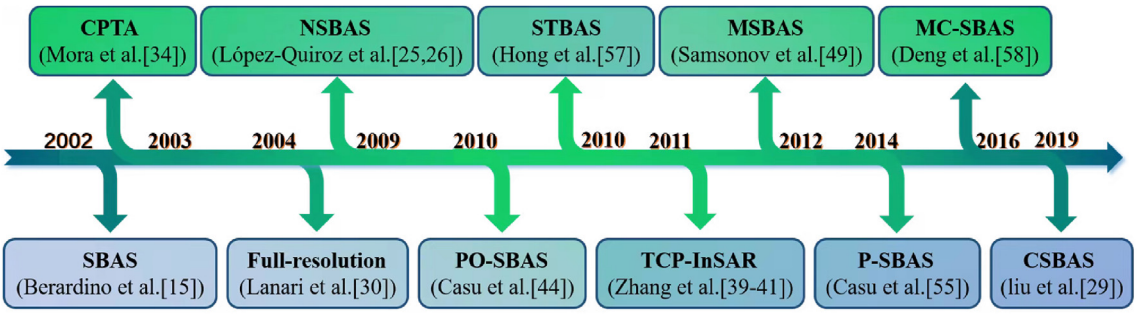

Fig. 4. Several main improved SBAS methods.

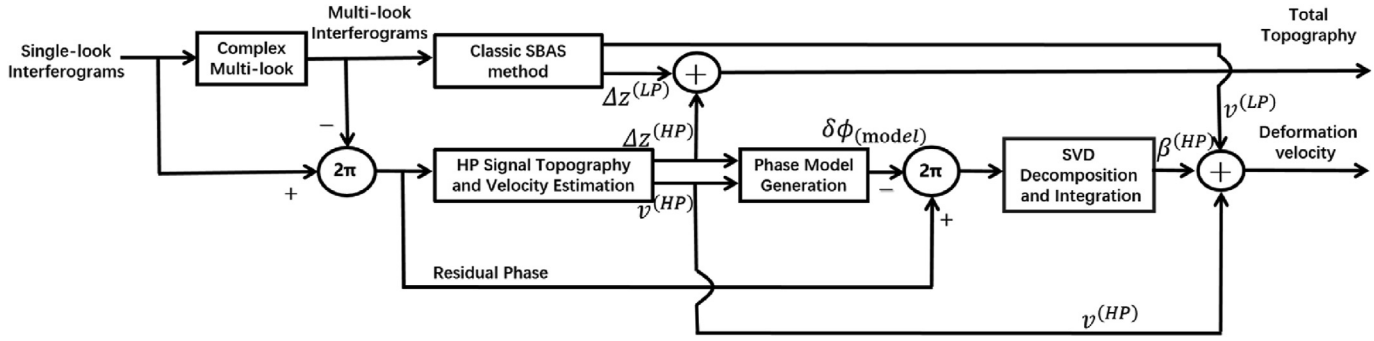

Fig. 5. Block diagram of the full-resolution SBAS method (this plot is adapted from [30]). The plus and minus signs beside the broken line with arrows respectively indicate whether the phase component is needed and removed in the next step. And the plus signs in a circle mean the sum of several different components.

with high coherence in that layer only. The process of choosing the points and layers is described below. For any pixel (x, y), when the number of interferograms with an unwrapping phase at that pixel is larger than a certain threshold M, this pixel is determined as a high-coherence point. For each high-coherence point, we only use the interferogram with the unwrapping phase to construct the error Equation (4), which means that the error equation of each high coherence point is different. To verify the accuracy of the ISBAS method, Gee et al. [33] used this method to obtain the time-series deformation of natural gas production and geological storage areas in the north Netherlands. The accuracy, within 1.52 mm/year and 1.12 mm/year, is equivalent to that of the PSI. The ISBAS method is suitable for monitoring the deformation of a natural surface. Compared with the classic SBAS method, the density of the selected points is significantly increased, as shown in Fig. 6.

In addition, temporarily coherent point SAR interferometry (TCP-InSAR) also proposed the selection of high coherence points based on the pixel offset (refer to the next section for details). In conclusion, the above three methods increase the density of HP selection and describe more deformation details than the classic SBAS method. However, in actual applications, an appropriate method should be selected according to different application scenarios.

3.3. Improving the accuracy of monitoring deformation

Compared with the SBAS method, the PSI method can better avoid atmospheric and orbital errors. Simultaneously, the three-dimensional phase unwrapping used by PSI is more accurate than the traditional two-dimensional one. Therefore, it is crucial to combine the advantages of these two methods. Presently, the following two representative combined methods of PSI and SBAS have been developed.

3.3.1. Coherent point target analysis (CPTA)

CPTA is a time-series InSAR technique that combines the PSI and SBAS methods. Mora et al. [34] proposed this technique for the first time and applied it to the deformation monitoring of Catalonia, Spain. The results showed that an accurate surface displacement could be obtained using only seven SAR images in this area. The core ideas of this method are as follows. First, the high coherence candidates were selected from the average coherence of all interferograms. The resulting non-uniform mesh is tessellated with Delaunay triangulation to establish connections among these high coherence candidates. The differences in the linear component of movement and residual DEM error are estimated by maximizing the model coherence coefficient at each arc and integrating to

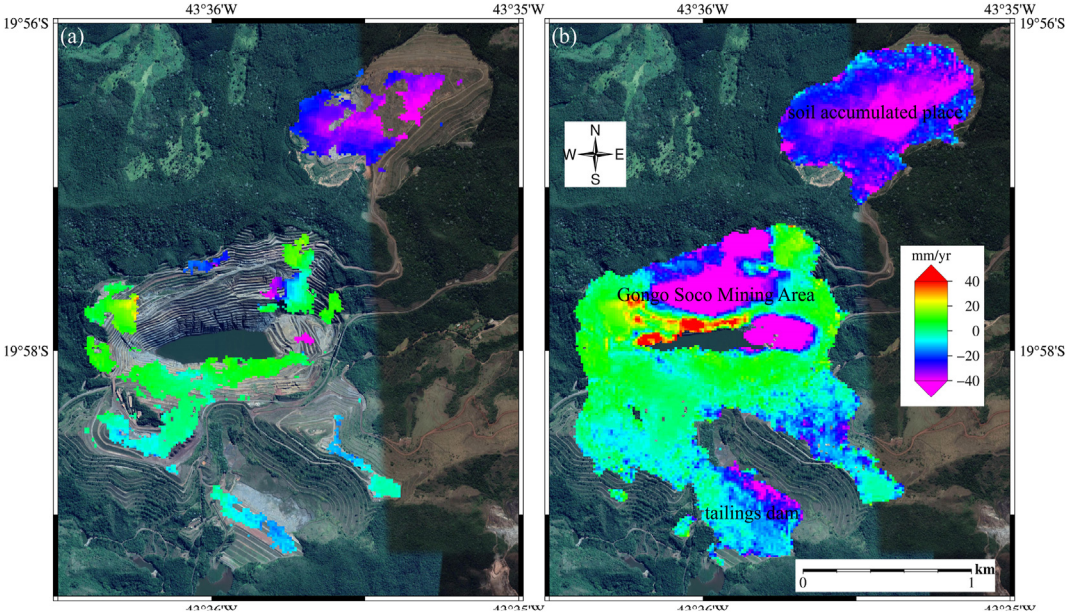

Fig. 6. Ground deformation velocity map using (a) the classic SBAS and (b) ISBAS methods over a mining region in Brazil.

obtain the absolute linear deformation rate and elevation residual. Subsequently, the residual differential phase, in which the linear deformation and residual DEM error are removed from the interferograms, is used to calculate the nonlinear movement component with spatio-temporal filtering. Finally, the sum of the linear and nonlinear deformation phases is the accurate ground deformation phase, where the nonlinear deformation phase includes high- and low-pass signals. When SAR images in a study area are less, this method can obtain more accurate deformation information without prior information. Therefore, it has been widely used to monitor the deformation of landslides, land subsidence, mining, etc. [35–38].

3.3.2. Temporary coherent point SAR interferometry(TCP-InSAR)

Zhang et al. [39–41] proposed another SBAS technique based on temporary coherent points by combining the PSI and SBAS methods. The core idea of this method is that the characteristics of strong scatterers are not sensitive to the window size and oversampling factor used in image registration. Analyzing the standard deviation of the point target offset during the image registration process determines whether it is a coherent point. When the standard deviation is less than a certain threshold, the point target is regarded as a temporary coherent point (TCP). The assumption that N offsets OT_j is obtained on the TCP candidate point j; if the standard deviation of the set of offsets is less than 0.1 pixels, the candidate point j is considered as a TCP point, namely:

$$\begin{aligned} &O\mathbf{T_j} = \left[ot_{j1}\ \ ot_{j2}\ \ \ldots\ \ ot_{jN}\right] \\ &std\left(O\mathbf{T_j}\right) < 0.1 \end{aligned} \tag{5}$$

After selecting the TCP points, a local Delaunay triangulation network was constructed, and the least-squares method was used to obtain the velocity difference term among these TCP points. Finally, the least-squares solution is applied to the velocity difference term to retrieve the actual deformation rate. The TCP-InSAR method is beneficial in increasing the density of the selected points by utilizing the offset's standard deviation. It is widely used in landslide deformation monitoring and land subsidence [42]. In addition, Liu et al. [43] used interferograms with extremely short spatial baselines to simplify TCP-InSAR modeling and parameter estimation. This method increases the density of selected points and is suitable for monitoring deformation when only a small number of SAR images are available.

In conclusion, the combined PSI and SBAS is suitable for monitoring the deformation of a local area and can achieve high accuracy. However, because of the extensive calculation, these methods cannot be applied to monitor large-area deformation.

3.4. Measuring the multi-dimensional deformation

The classic D-InSAR and SBAS methods can only measure the one-dimensional deformation of the radar line of sight. In fact, the monitored deformation is the projection of the actual ground three-dimensional deformation in the direction of the radar's line of sight. When the ground object moves in a direction perpendicular to the line of sight, the classic SBAS method cannot detect ground displacement at all. Therefore, it is essential to realize the multi-dimensional time-series deformation monitoring of ground displacement. Compared with PSI, the SBAS method is more flexible and more suitable for monitoring time-series multi-dimensional ground deformation. Therefore, two methods have been developed.

3.4.1. Pixel-offset SBAS(PO-SBAS)

To obtain the multi-dimensional time-series motion of a ground target with a relatively violent movement, Casu et al. [44] developed a two-dimensional pixel-offset SBAS(PO-SBAS) method in 2011. PO-SBAS is a method that calculates deformation based on the amplitude information of a pixel. The realization of this method is divided into the following processes: First, the amplitudes of the selected image pairs are exploited to calculate the relative across-track (range) and along-track (azimuth) pixel-offsets (PO). The SBAS inversion strategy is then applied to retrieve the time-series range and azimuth displacement at each moment. To describe the ground displacement more accurately, Casu et al. [45] used pixel offsets from ascending and descending SAR images to retrieve the time-series three-dimensional deformation. Notably, this method pairs ascending and descending acquisitions that are as close as possible in time to consider them as acquired simultaneously. The PO-SBAS method is mainly used to monitor volcanic movement [44], landslides [46] and other relatively violent deformations. However, traditional offset calculation methods produce a large amount of calculation for fast-moving earth surfaces (such as glaciers, which may move tens to hundreds of meters per year). To solve this problem, Leonardo et al. [47] first predicted the pixel position from the image using the speed obtained from the short-term interferogram and then calculated the pixel offset with a small search window, which improved the calculation efficiency.

Unfortunately, unlike the high-precision deformation measurement based on phase information, the PO-SBAS based on amplitude information is challenging to monitor the slow, sustained three-dimensional surface deformation [48].

3.4.2. Multidimensional SBAS (MSBAS)

In 2012, Samsonov et al. [49] developed the MSBAS method to obtain multidimensional time-series deformation in another way. Unlike PO-SBAS, MSBAS calculates deformation based on the differential interferogram phase. This method uses time-series SAR images of ascending and descending orbits and unifies their acquisition time on the same timeline by a temporal compensation factor. Subsequently, it uses the least-squares method to solve the east-west and vertical directions by adding temporal regularization constraints. This method is suitable for obtaining two-dimensional horizontal and vertical deformations related to land subsidence, such as mining [50], urban development [51], carbon sequestration, accumulation and growth of permafrost, and volcanic activity. However, it is not suitable for studies where there may be a sizeable N–S displacement component. Furthermore, Samsonov et al. [52,53] extended from two-to three-dimensional MSBAS by adding restrictions on the movement of glaciers and landslides along the surface. In addition, Guo et al. [54] used the pixel offset tracking method to obtain the azimuth and range displacement and unified its acquisition date on the same timeline using a temporal compensation factor. They developed a PO-MSBAS method by combining PO-SBAS and MSBAS.

3.5. Other SBAS-related methods

In addition to the various methods mentioned above, Casu et al. [55] proposed parallel SBAS(P-SBAS) technology, which improved the solution efficiency of the classic SBAS method. Subsequently, Luca et al. [56] transplanted the P-SBAS method to the Amazon cloud computing environment to obtain two-dimensional time-series deformation in Southern California, which significantly

improved the operating efficiency. Moreover, to improve the time resolution of the deformation monitoring, Hong et al. [57] proposed a small temporal baseline subset (STBAS) for integrating multi-temporal and multitrack data in 2010. This method provides a basis for studying refined deformation modes over time. Additionally, a multi-platform long-time sequence SBAS(MC-SBAS) method was proposed by Deng et al. [58], which provided an idea for long-term deformation monitoring. Some other SBAS methods will not be introduced here.

Different SBAS methods have different accuracy and are suitable for different application scenarios. Their accuracy levels are mainly divided into four categories: Firstly, the Full-resolution SBAS, CPTA, TCP-InSAR have relatively higher accuracy, since they remove or avoid inherent error phase more finely; Secondly, the accuracy of ISBAS, P-SBAS, STABS is the same as the classic SBAS method, because their primary purpose is to improve Spatio-temporal resolution and computational efficiency; Thirdly, the precision of NSBAS, CSBAS, MSBAS, MC-SBAS is limited by the accuracy of the constraint. Finally, the accuracy of PO-SBAS could be slightly lower than the classic SBAS method because the calculated displacement based on the intensity information is far less accurate than phase information. We briefly summarize the SBAS methods mentioned above, as presented in Table 1. Readers can choose the appropriate SBAS method according to the actual situation.

4. Applications

4.1. Monitoring of ground subsidence

Ground subsidence is a common geological disaster. The occurrence of ground subsidence has severely damaged infrastructure construction and can cause significant economic losses. The causes of surface subsidence are mainly divided into natural and human factors. Natural factors include precipitation [59], viscosity characteristics of the soil layer [60], and distribution of fault zones [61]. Human factors mainly exploit underground resources [33,59,62] and changes in ground load [63]. The SBAS method is widely used to monitor ground subsidence, including three application scenarios: urban, linear infrastructure, and mining areas.

4.1.1. Ground subsidence of urban

Because there are many artificial buildings in the city, they have relatively stable scattering characteristics, which facilitate the application of the SBAS method. For example, Morishita et al. [64] used LiCSBAS to detect two-dimensional time-series deformation fields for 73 major cities in Japan, as shown in Fig. 7. The results showed that linear subsidence occurred in Hirosaki, Kujukuri, Niigata, and Kanazawa, episodic subsidence occurred in Sanjo, and linear uplift occurred in Chofu. As for the causes, the urban's ground subsidence is closely related to groundwater level changes in most cases [65]. For example, Zhou et al. [66] analyzed the impact of different land-use types on ground subsidence and found that subsidence was more evident in areas where industrial and agricultural water consumption was significant. Further, Chaussard et al. found that there may be a lag effect between the change in groundwater level and ground subsidence [67]. Other reasons include soil properties [68,69], karst dissolution of subsurface carbonate rocks [59], ground load [70], etc.

Many studies have utilized the SBAS method to monitor urban settlements and explore its mechanisms. However, the following two problems still exist. First, as the resolution of SAR images increases, the dense distribution of buildings aggravate the phenomenon of foreshortening, layover, and radar shadow, which negatively affect the final time-series deformation result. There are relatively few quantitative analyses on ground subsidence and groundwater seepage characteristics, which is also a crucial issue that needs to be solved in the future.

Table 1
The primary several improved SBAS methods and their advantage.

Aspects	Main method	Advantage
Solving the ill-posed equation	NSBAS/CSBAS/ other constraint	Solve rank deficit and ill-conditioned problems
Increasing the HPs density	Full-resolution SBAS/ ISBAS	Improve HPs' density
Improving the accuracy	CPTA/ TCP-InSAR	Reduce noise impact and improve solution accuracy
Measuring the multidimensional deformation	PO-SBAS/	Monitor rapid multidimensional deformation
	MSBAS	Monitor slow multidimensional deformation
	P-SBAS	High computational efficiency
Other SBAS-related methods	STABS	High temporal resolution
	MC-SBAS	Long-term monitoring

4.1.2. Ground subsidence of mining area

The mining process of underground mineral resources changes the original stress balance of the soil, resulting in ground collapse or a large-area subsidence funnel. Owing to the large deformation rate in the mining area, the SBAS method has irreplaceable advantages compared to other time-series InSAR technologies. Nowadays, a lot of research based on the SBAS method has also been carried out in mining areas. For example, Baek et al. [71] used the SBAS method to obtain the cumulative deformation of several mining areas in the Samchuk coalfield from 1992 to 1998, and found that ground subsidence occurred above the excavation and fault line. Compared with one-dimensional deformation, multidimensional deformation can better reveal the deformation characteristics. For example, Samsonov et al. [50] used MSBAS to obtain a two-dimensional deformation field in the Luxembourg area related to coal mining. Notably, Li et al. [72] used an a priori mining deformation model to obtain three-dimensional deformation results based on a single radar line-of-sight deformation for the first time. This method opened a new chapter for the use of single-track SAR data to monitor three-dimensional displacement. Subsequently, Yang et al. [73] extended the technique to obtain the time-series three-dimensional deformation of the Datong and Daliuta mining areas in Shanxi.

Because most mining areas have significant deformation rates, it is difficult to cause temporal decorrelation effects. Therefore, it is difficult to monitor the deformation of mining areas. With the continuous launch of longer-band SAR satellites and the improvement of the spatio-temporal resolution, the deformation monitoring accuracy of mining areas will be significantly improved in the future.

4.1.3. Ground subsidence of linear infrastructure

Linear infrastructure, such as roads, railways, and underground pipe networks, is essential for social and economic development. The over-exploitation of underground resources has caused uneven subsidence of the ground, posing a potential threat to the operation of linear infrastructure. Because linear infrastructure is relatively narrow, high-resolution SAR images are required to monitor their displacement. With the launch of a series of high-resolution SAR satellites, it has become possible to use the SBAS method to obtain the ground displacement of linear infrastructure. For example, Rao et al. [74] used 40 scenes of Cosmo-SkyMed images to retrieve the time-series deformation of a newly built high-speed railway in southeast China.

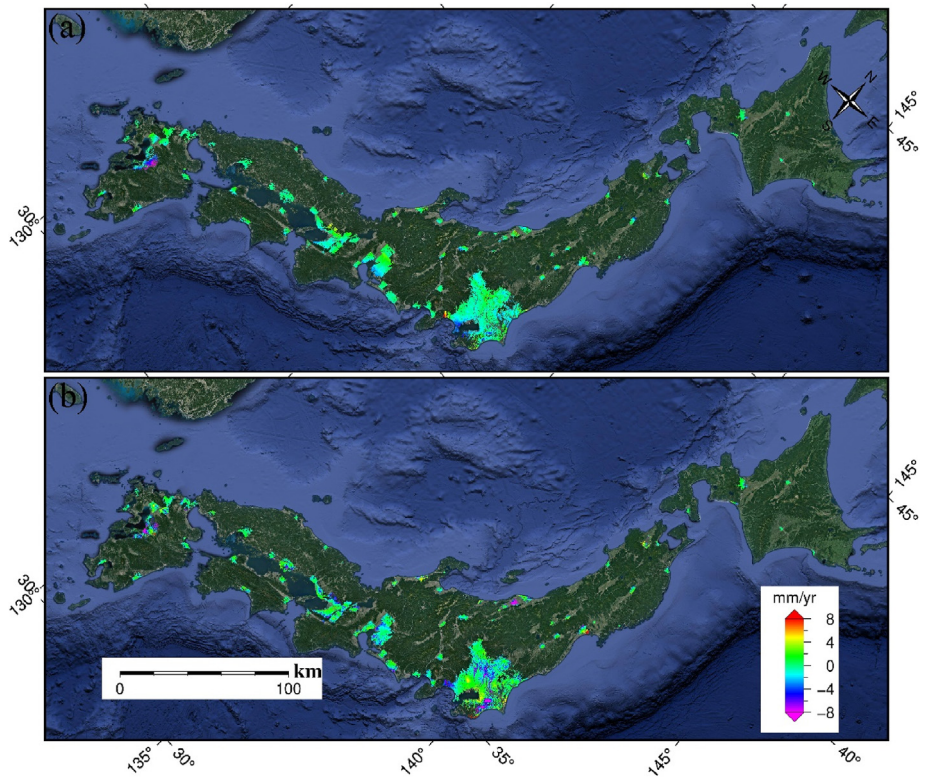

Fig. 7. East-west and vertical deformation velocity map covering the major cities in Japan from 2014 to 2020 using the LiCSBAS software. (a) and (b) represent the average deformation rate in the east-west and vertical directions from 2014 to 2020(the data derived from [64]), respectively.

Presently, the deformation monitoring of linear infrastructure faces two main difficulties. First, when a linear infrastructure is located in a vegetation coverage area, it is difficult to use the SBAS method to effectively measure its displacement owing to the temporal decorrelation effect. Another difficulty is that it is challenging to obtain the monitoring deformation of ultra-long-distance linear infrastructure. The simultaneous meeting of both high-resolution and large-area deformation measurement requirements is a critical problem.

4.2. Monitoring of seismic activity

Monitoring seismic activity is an outstanding and successful application in InSAR applications. Because D-InSAR was applied to deformation observations of the Landers earthquake in 1993 [4], much research has been conducted on co-seismic deformation. In the intermediate period between the occurrence of two earthquakes, there was a slow stress accumulation process. This period is referred to the inter-seismic period. Monitoring the deformation during the inter-seismic period is difficult. This is mainly due to the small and widely distributed characteristics of inter-seismic deformation. An inter-seismic displacement signal can be masked by the orbit error and atmosphere [75]. To correctly separate the inter-seismic deformation and orbit error, Biggs et al. [76] proposed a polynomial network method to remove the orbit error by considering the network configuration of the interferogram. They obtained the inter-seismic deformation field in Denali, Alaska, and deduced that the slip rate in this area was approximately 10.5 ± 5.0. Subsequently, Bigg, Elliott, and Wang et al. [76–78] developed a PIRATE toolkit for monitoring inter-seismic deformation based on the network method. Currently, this toolkit is widely used to monitor inter-seismic deformation. Additionally, owing to the difficulty in monitoring inter-seismic deformation, a variety of algorithms has been developed. For example, Cavalié and Jolivet et al. [79,80] used a noise function to select excellent quality unwrapping interferograms. Hussain et al. [81] used an iterative unwrapping method to improve the accuracy of unwrapping interferograms. Although different researchers have used different methods to obtain inter-seismic deformation, there is no universal method for obtaining the deformation.

Unlike inter-seismic deformation, post-seismic deformation occurs after an earthquake. Post-seismic deformation is relatively easier to obtain compared to inter-seismic deformation. The SBAS method has been widely used in the monitoring of post-seismic deformation, such as the M_W6.8 Bam earthquake [82], M_W7.8 Gorkha earthquake [83], M_W7.8 Kokoxili earthquake [84], and California Earthquake [85]. Currently, three main mechanisms have been used to explain post-seismic deformation: slip, viscoelastic relaxation, and poroelastic relaxation. However, none of these mechanisms can adequately explain all post-seismic deformation. In most cases, the three mechanisms mentioned above occur simultaneously in an earthquake. Therefore, it is crucial to understand the mechanisms that play a leading role in post-seismic deformation.

4.3. Monitoring of landslide

Landslides are a typical type of geological disaster, which are defined as rocks and soil moving along a slope. The SBAS method was used to monitor landslide movement, including landslide position and displacement. For example, Zhao et al. [86] used multi-temporal ALOS/PALSAR images to obtain more than 50 active landslides and their deformation in northern California and southern Oregon based on the SBAS method. The results show that

landslide movement is related to precipitation, and there is a lag period of 1–2 months between the peak precipitation and the maximum landslide displacement. In general, ISBAS and TCP-InSAR are often used to monitor the one-dimensional deformation of landslide areas [87,88]. However, in most cases, it is difficult for the traditional one-dimensional LOS deformation to reflect the actual movement of the landslide. To obtain the multi-dimensional time-series deformation of the landslide area, Sun et al. [89] used PO-SBAS to retrieve the two-dimensional time-series deformation of the Tanjiahe landslide in the Three Gorges area.

However, landslides in areas covered by lush vegetation remain challenging to monitor. Owing to spatio-temporal decorrelation, atmospheric phase screens, and artifacts caused by near-surface moisture changes, it is difficult to map and monitor landslides in forest areas. In the future, the launch of more long-band satellites and the effective use of multi-polarization information may help solve this problem.

4.4. Monitoring of permafrost activity

Permafrost is a vital part of the cryosphere, and the uppermost part is the active layer. The active layer has the characteristics of frost heave and thaw settlement. Therefore, the freeze–thaw cycle in permafrost regions will produce extensive ground deformation, affecting human engineering activities and infrastructure [90]. The classical SBAS method often uses linear models to describe ground displacement. In fact, the causes of frozen soil deformation are complex. Linear models cannot accurately portray the surface deformation process [91]. Therefore, selecting an appropriate deformation model has become a vital issue for monitoring the deformation of permafrost. Presently, several major models have been developed that include models that consider the accumulation time of frozen soil thawing settlement [92], combining linear and periodic functions [90], cubic power function [93], integrating external factors (such as climate), and internal factors (such as tectonic activity and thermal characteristics of permafrost) [94]. To study the lag between the deformation of frozen soil and temperature, Zhao et al. used the one-dimensional heat conduction equation for the first time in the study of permafrost [94]. Although the SBAS method has broad application potential in frozen soil research, its use in inverting active layer parameters is still an important issue and difficult point [95].

4.5. Monitoring of glacier movement

With global warming and the impact of human activities, glacier movement has accelerated. Subsequently, secondary disasters caused by glacier movement are frequent. Because the InSAR technique has a strong penetrating ability and is not affected by clouds and rain, it has a considerable advantage over optical remote sensing in monitoring glacier movement. Simultaneously, the SBAS method significantly avoids the temporal–spatial decorrelation effect by selecting a shorter temporal–spatial baseline interference pair, which provides convenience for monitoring the time-series deformation of glacier movement. However, the glacier displacement was vertical and horizontal. The classic SBAS method, which can only measure the deformation of the radar line of sight, is no longer applicable [96]. Therefore, Samsonov et al. [52] used the MSBAS method for the first time to obtain the three-dimensional time-series deformation of the glacier by adding the movement conditions of the glacier's displacement along the surface. In fact, the movement rate of most glaciers is so fast that it is difficult to accurately detect the deformation using conventional D-InSAR methods. More time-series analysis methods based on offset tracking methods have been applied to monitor glacier movement; for instance, Euillades, Li et al. [20,47] used PO-SBAS technology to obtain the two-dimensional and three-dimensional time series motion of glaciers. This proves that the PO-SBAS method is suitable for large glacier displacements. In 2020, Guo et al. [54] monitored the activities of the Hispar Glacier using PO-MSBAS, as illustrated in Fig. 8. However, using the SBAS method to obtain the multidimensional deformation of glaciers requires the integration of multi-source data. The weight ratio is significant in the data fusion process. This will be a key and challenging point of future research [97].

4.6. Monitoring of volcanic activity

It is difficult for conventional geodesy to conduct research on large-area volcanic deformation characteristics. However, the SBAS method is very suitable for measuring complex surface deformation caused by volcanic dike invasion, magma sac expansion and contraction, and geothermal systems. Since it was proposed in 2002, the SBAS method has been used to monitor the volcanic deformation of Campi Flegrei in southern Italy [15]. To better describe the movement of the volcano, Manconi et al. [98] combined the classic SBAS method and PO-SBAS to obtain time-series displacements of the Fernandina and Sierra Negra volcanoes. The results show that this method can significantly increase the measured spatial density and better constrain the magma source volume change. We successfully observed the surface deformation of at least 160 volcanoes using InSAR. Owing to the complex deformation mechanism of volcanoes, the combination of ground deformation and models to accurately estimate the specific physical parameters of the underground magma pocket is still an important issue.

5. Current challenges

5.1. Monitoring displacement in low-coherence areas

Owing to the influence of different satellite flight postures, the electromagnetic reflection characteristics of the Earth's surface target scatterers change, and the radar echo signal is affected by different degrees of spatio-temporal decoherence. When there is no linear correlation between the two signals, complete decoherence occurs. Two situations are likely to cause the generation of decoherent noise. First, the reflection characteristics of vegetation are extremely prone to change owing to its growth over time. Therefore, the vegetation coverage area is a typical low coherence area. Second, a deformation exceeding a certain magnitude in a short period also leads to decoherence. The phenomenon of decoherence can easily result in unwrapping errors and inaccurate subsequent deformation analyses. Two typical methods are commonly used to obtain time-series displacement in the low-coherence region. 1) The corner reflector is placed in the low-coherence area to increase the density of the high-coherence points. However, the corner reflector is costly, and it is not easy to obtain the historical deformation before the corner reflector is installed [99]. 2) The deformation is obtained by pixel offset tracking (POT) [100] or multi-aperture radar interferometry (MAI) [101]; however, the accuracy of the deformation results obtained by the two methods is relatively low. It is challenging to meet the high-precision requirements for the time-series deformation monitoring of slow ground displacement.

5.2. Estimation of atmospheric phase

The atmospheric effect is an essential error source in the current InSAR technique. There are some differences in weather conditions

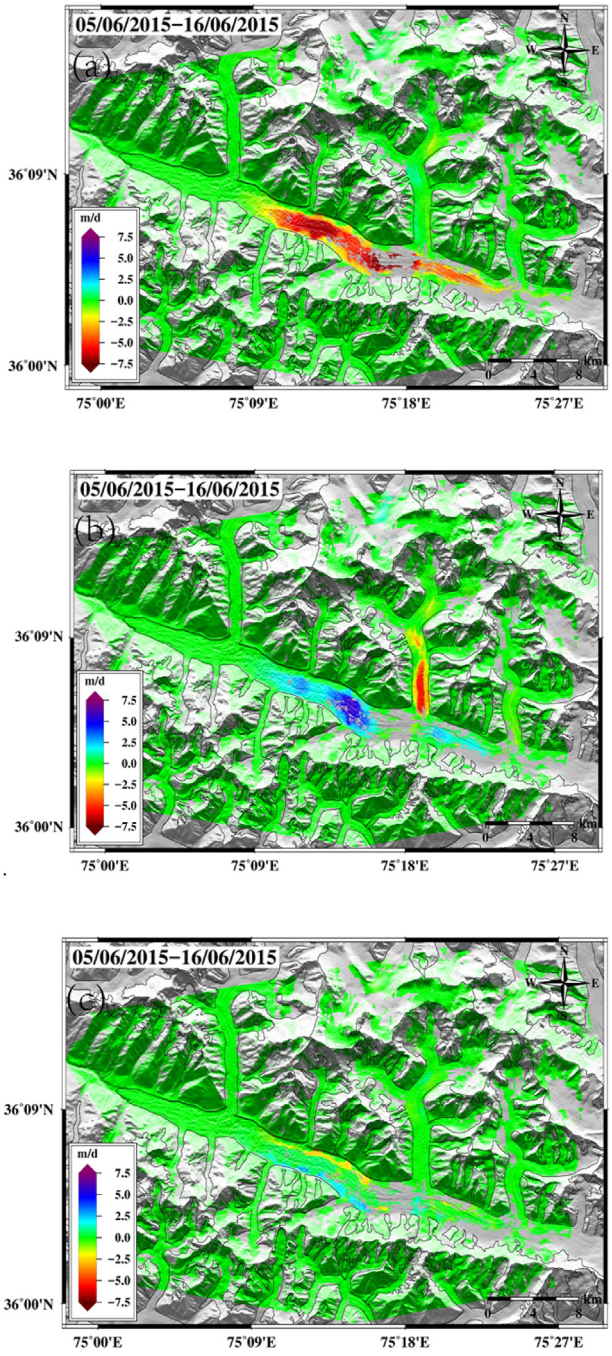

Fig. 8. **(a), (b),** and **(c)** represent the average deformation rate in the east-west, north-south, and vertical directions using the PO-MSBAS method (the data derived from [54]), respectively.

when electromagnetic wave signals pass through the atmosphere at different times, resulting in the so-called "atmospheric delay". This is mainly due to two factors: the troposphere and ionosphere. Generally, the ionosphere has a more noticeable impact on the L-band than the C-band. This effect is more evident in the polar regions. Because the phase delay caused by the ionosphere is rarely encountered, most previous InSAR studies only considered removing the tropospheric atmospheric delay effect. With the launch of more long-wavelength satellites, it is critical to remove the delay effect caused by the ionosphere. The tropospheric atmospheric delay is mainly composed of two parts: a stratified atmosphere and atmospheric turbulence. Generally, the stratified atmosphere phase is removed by the following three methods: (1) The removal is performed by introducing an external atmospheric correction product, but the method is limited by the temporal–spatial resolution and accuracy of the external data [102–104]. (2) Exploring the correlation between ground elevation and the atmospheric delay phase is a common processing strategy. However, this method requires prior knowledge of the functional relationship between elevation and atmospheric delay [105], and it can remove some deformation signals. (3) Difference processing uses adjacent stable point phases to avoid atmospheric influence, but the method is limited by the density of the high coherence points [39]. To correct the turbulent atmosphere, it is usually assumed that the atmospheric delay phase caused by atmospheric turbulence appears to be random in time. This part of the atmospheric delay phase is often processed by the temporal high-pass and spatial low-pass filtering methods used in SBAS methods. The premise of the filtering method to remove the delay effect caused by atmospheric turbulence is to assume that it obeys a Gaussian distribution, which is often not in line with the actual situation.

5.3. Data processing in the big data era

Presently, InSAR data processing has entered the era of big data. (1) The continuous launch of SAR satellites has significantly enriched InSAR data sources; (2) it provides a framework for massive data processing owing to the rise of big data science and artificial intelligence. In the big data era, the SBAS method also faces some challenges. First, with the continuous acquisition of SAR data, one important issue is how to achieve real-time surface deformation monitoring by combining the previous deformation results with the subsequently acquired SAR images. Second, the new generation of SAR satellites is characterized by multi-polarization, multi-mode, and multi-channel. However, the SBAS method currently only uses single-polarization, single-mode, and single-channel information. Therefore, it is vital to use all satellite information to improve the accuracy of the current SBAS method effectively. Finally, the current monitoring means of large-area and time-series multidimensional deformation cannot be effectively integrated. Therefore, breaking through this limit will provide technical support for time-series three-dimensional deformation monitoring on a national or even global scale.

In the big data era, the SBAS method may develop in the following ways: (1) With the help of big data analysis and deep learning, InSAR errors will be effectively separated. Deep learning will be applied to phase unwrapping and pay more attention to retrieving time-series deformation. (2) It is also an essential direction of the SBAS method to realize the integration of large-area, long-term sequence, and three-dimensional deformation monitoring technology based on the P-SBAS method and cloud computing platforms such as the Google Earth Engine. (3) The fusion of traditional geodetic data, optical images, and SAR data has become a new trend in understanding the disaster mechanism further. Simultaneously, it is necessary to construct a real-time disaster monitoring and warning system by integrating time-series InSAR and GIS technology.

6. Conclusions

Since the SBAS method was proposed in 2002, various improved SBAS methods have been developed, and their applicability for monitoring deformation has been continuously enhanced. Several different SBAS approaches are described in this paper, but the number will undoubtedly increase in the future. The technical

improvements achieved so far concern all main SBAS components:(a) solving the ill-posed equation, (b) increasing the density of high-coherence points, (c) improving the accuracy of monitoring deformation, (d) measuring the multidimensional deformation and (e) other SBAS-related methods. The potential of the SBAS technique can be highlighted from these broad spectra of SBAS applications, such as ground subsidence, seismic activity, landslides, permafrost degradation, glacier movement, and volcanic activity. However, the SBAS method also faces a series of problems, such as deformation measurement in low-coherence regions, estimation of atmospheric errors, and data processing in the big data era. In the big data era, the SBAS method will be developed for high-precision, large-area, long-time sequences, and real-time surface deformation monitoring.

Conflicts of interest

The authors declare that there is no conflicts of interest.

Acknowledgment

We thank the reviewers for their helpful comments. This work was funded by the National Key R&D Program of China (2019YFC1509205), the National Natural Science Foundation of China (Nos. 42174023 and 41804015), the Postgraduate Scientific Research Innovation Project of Hunan Province (150110074) and the Postgraduate Scientific Research Innovation Project of Central South University (212191010).

References

[1] A. Rogers, R.V. Ingalls, Mapping the surface reflectivity by radar interferometry, Science 165 (1969) 797–799.
[2] H.A. Zebker, R.M. Goldstein, Topographic mapping from interferometric synthetic aperture radar observations, J. Geophys. Res. Solid Earth 91 (1986) 4993–4999.
[3] A.K. Gabriel, R.M. Goldstein, H.A. Zebker, Mapping small elevation changes over large areas: differential radar interferometry, J. Geophys. Res. Solid Earth 94 (1989) 9183–9191.
[4] D. Massonnet, M. Rossi, C. Carmona, F. Adragna, G. Peltzer, K. Feigl, T. Rabaute, The displacement field of the Landers earthquake mapped by radar interferometry, Nature 364 (1993) 138–142.
[5] Z. Lu, T. Masterlark, D. Dzurisin, Interferometric synthetic aperture radar study of Okmok volcano, Alaska, 1992–2003: magma supply dynamics and postemplacement lava flow deformation, J. Geophys. Res. Solid Earth 110 (2005).
[6] R.M. Goldstein, H. Engelhardt, B. Kamb, R.M. Frolich, Satellite radar interferometry for monitoring ice sheet motion: application to an Antarctic ice stream, Science 262 (1993) 1525–1530.
[7] C. Carnec, C. Delacourt, Three years of mining subsidence monitored by SAR interferometry, near Gardanne, France, J. Appl. Geophys. 43 (2000) 43–54.
[8] X. Ding, G. Liu, Z. Li, Z. Li, Y. Chen, Ground subsidence monitoring in Hong Kong with satellite SAR interferometry, Photogramm. Eng. Rem. Sens. 70 (2004) 1151–1156.
[9] H.A. Zebker, J. Villasenor, Decorrelation in interferometric radar echoes, IEEE Trans. Geosci. Rem. Sens. 30 (1992) 950–959.
[10] R.F. Hanssen, Radar Interferometry: Data Interpretation and Error Analysis, Vol. 2, Springer Science & Business Media, 2001.
[11] D.T. Sandwell, E.J. Price, Phase gradient approach to stacking interferograms, J. Geophys. Res. Solid Earth 103 (1998) 30183–30204.
[12] A. Ferretti, C. Prati, F. Rocca, Nonlinear subsidence rate estimation using permanent scatterers in differential SAR interferometry, IEEE Trans. Geosci. Rem. Sens. 38 (2000) 2202–2212.
[13] A. Ferretti, C. Prati, F. Rocca, Permanent scatterers in SAR interferometry, IEEE Trans. Geosci. Rem. Sens. 39 (2001) 8–20.
[14] S.A. Usai, New Approach for Longterm Monitoring of Deformations by Differential SAR Interferometry, 2001.
[15] P. Berardino, G. Fornaro, R. Lanari, E. Sansosti, A new algorithm for surface deformation monitoring based on small baseline differential SAR interferograms, IEEE Trans. Geosci. Rem. Sens. 40 (2002) 2375–2383.
[16] F. Xue, X. Lv, F. Dou, Y. Yun, A review of time-series interferometric SAR techniques: a tutorial for surface deformation analysis, IEEE Geosci. Rem. Sens. Mag. 8 (2020) 22–42.
[17] F. Casu, M. Manzo, R. Lanari, A quantitative assessment of the SBAS algorithm performance for surface deformation retrieval from DInSAR data, Remote Sens. Environ. 102 (2006) 195–210.
[18] P. Berardino, G. Fornaro, R. Lanari, E. Sansosti, A new algorithm for surface deformation monitoring based on small baseline differential SAR interferograms, 2002. Available online, https://scholar.google.com.hk/citations?user=_K6MiXAAAAAJ&hl=zh-CN&oi=sra.
[19] D. Yunkai, W. Yu, Z. Heng, W. Wei, L. Dacheng, Yu. Wang, Forthcoming spaceborne SAR development, J. Radars. 9 (2020) 1–33, https://doi.org/10.12000/JR20008.
[20] J. Li, Z.-W. Li, L.-X. Wu, B. Xu, J. Hu, Y.-S. Zhou, Z.-L. Miao, Deriving a time series of 3D glacier motion to investigate interactions of a large mountain glacial system with its glacial lake: use of Synthetic Aperture Radar Pixel Offset-Small Baseline Subset technique, J. Hydrol. 559 (2018) 596–608.
[21] C. Werner, T. Strozzi, U. Wegmüller, Deformation time-series of the lost-hills oil field using a multi-baseline interferometric SAR inversion algorithm with finite-difference smoothing constraints, Trans. Geosci. Rem. Sens. 40 (2002) 2375–2383.
[22] J. Zhaoying, L. Guolin, T. Qiuxiang, Regularization solution of small baseline subset deformation model inversion, Acta Geod. Cartogr. Sinica 45 (2016) 566–573+600.
[23] T.R. Lauknes, H.A. Zebker, Y. Larsen, InSAR deformation time series using an L_1-norm small-baseline approach, IEEE Trans. Geosci. Rem. Sens. 49 (2010) 536–546.
[24] D.A. Schmidt, R. Bürgmann, Time-dependent land uplift and subsidence in the Santa Clara valley, California, from a large interferometric synthetic aperture radar data set, J. Geophys. Res. Solid Earth 108 (2003).
[25] P. López-Quiroz, M.-P. Doin, F. Tupin, P. Briole, J.-M. Nicolas, Time series analysis of Mexico City subsidence constrained by radar interferometry, J. Appl. Geophys. 69 (2009) 1–15.
[26] M.-P. Doin, S. Guillaso, R. Jolivet, C. Lasserre, F. Lodge, G. Ducret, R. Grandin, Presentation of the small baseline NSBAS processing chain on a case example: the Etna deformation monitoring from 2003 to 2010 using Envisat data, in: Proceedings of the Proceedings of the Fringe Symposium, 2011, pp. 3434–3437.
[27] Y. Morishita, M. Lazecky, T.J. Wright, J.R. Weiss, J.R. Elliott, A. Hooper, LiCSBAS: an open-source InSAR time series analysis package integrated with the LiCSAR automated sentinel-1 InSAR processor, Rem. Sens. 12 (2020) 424.
[28] S. Usai, A least squares database approach for SAR interferometric data, IEEE Trans. Geosci. Rem. Sens. 41 (2003) 753–760.
[29] Y. Liu, C. Zhao, Q. Zhang, Z. Lu, J. Zhang, A constrained small baseline subsets (CSBAS) InSAR technique for multiple subsets, Eur. J. Rem. Sens. 53 (2020) 14–26.
[30] R. Lanari, O. Mora, M. Manunta, J.J. Mallorquí, P. Berardino, E. Sansosti, A small-baseline approach for investigating deformations on full-resolution differential SAR interferograms, IEEE Trans. Geosci. Rem. Sens. 42 (2004) 1377–1386.
[31] C. Ojha, M. Manunta, R. Lanari, A. Pepe, The constrained-network propagation (C-NetP) technique to improve SBAS-DInSAR deformation time series retrieval, IEEE J. Sel. Top. Appl. Earth Obs. Rem. Sens. 8 (2015) 4910–4921.
[32] A. Sowter, L. Bateson, P. Strange, K. Ambrose, M.F. Syafiudin, DInSAR estimation of land motion using intermittent coherence with application to the South Derbyshire and Leicestershire coalfields, Remote Sens. Lett. 4 (2013) 979–987.
[33] D. Gee, A. Sowter, A. Novellino, S. Marsh, J. Gluyas, Monitoring land motion due to natural gas extraction: validation of the Intermittent SBAS (ISBAS) DInSAR algorithm over gas fields of North Holland, The Netherlands, Mar. Petrol. Geol. 77 (2016) 1338–1354.
[34] O. Mora, J.J. Mallorqui, A. Broquetas, Linear and nonlinear terrain deformation maps from a reduced set of interferometric SAR images, IEEE Trans. Geosci. Rem. Sens. 41 (2003) 2243–2253.
[35] L. Cascini, G. Fornaro, D. Peduto, Analysis at medium scale of low-resolution DInSAR data in slow-moving landslide-affected areas, ISPRS J. Photogrammetry Remote Sens. 64 (2009) 598–611.
[36] D. Ge, Y. Wang, L. Zhang, Y. Xia, X. Guo, Large scale land subsidence monitoring with a reduced set of SAR images, in: Proceedings of the 2009 IEEE International Geoscience and Remote Sensing Symposium, 2009, pp. IV-558–IV-561.
[37] K. Pawluszek-Filipiak, A. Borkowski, Integration of DInSAR and SBAS techniques to determine mining-related deformations using sentinel-1 data: the case study of rydułtowy mine in Poland, Rem. Sens. 12 (2020) 242.
[38] R. Tomás, Y. Márquez, J.M. Lopez-Sanchez, J. Delgado, P. Blanco, J.J. Mallorquí, M. Martínez, G. Herrera, J. Mulas, Mapping ground subsidence induced by aquifer overexploitation using advanced Differential SAR Interferometry: vega Media of the Segura River (SE Spain) case study, Remote Sens. Environ. 98 (2005) 269–283.
[39] L. Zhang, Z. Lu, X. Ding, H.-S. Jung, G. Feng, C.-W. Lee, Mapping ground surface deformation using temporarily coherent point SAR interferometry:

application to Los Angeles Basin, Remote Sens. Environ. 117 (2012) 429–439.
[40] L. Zhang, X. Ding, Z. Lu, Modeling PSInSAR time series without phase unwrapping, IEEE Trans. Geosci. Rem. Sens. 49 (2010) 547–556.
[41] L. Zhang, X. Ding, Z. Lu, Ground settlement monitoring based on temporarily coherent points between two SAR acquisitions, ISPRS J. Photogrammetry Remote Sens. 66 (2011) 146–152.
[42] Q. Sun, J. Hu, L. Zhang, X. Ding, Towards slow-moving landslide monitoring by integrating multi-sensor InSAR time series datasets: the Zhouqu case study, China, Rem. Sens. 8 (2016) 908.
[43] G. Liu, H. Jia, R. Zhang, Z. Li, Q. Chen, X. Luo, G. Cai, Ultrashort-baseline persistent scatterer radar interferometry for subsidence detection, ISPRS Ann. Photogram. Remote Sens. Sp Inform. Sci. 1 (2012) 41–48.
[44] F. Casu, A. Manconi, A. Pepe, R. Lanari, Deformation time-series generation in areas characterized by large displacement dynamics: the SAR amplitude pixel-offset SBAS technique, IEEE Trans. Geosci. Rem. Sens. 49 (2011) 2752–2763.
[45] F. Casu, A. Manconi, Four-dimensional surface evolution of active rifting from spaceborne SAR data, Geosphere 12 (2016) 697–705.
[46] A. Manconi, F. Casu, F. Ardizzone, M. Bonano, M. Cardinali, C. De Luca, E. Gueguen, I. Marchesini, M. Parise, C. Vennari, Brief communication: rapid mapping of landslide events: the 3 December 2013 Montescaglioso landslide, Italy, Nat. Hazards Earth Syst. Sci. 14 (2014) 1835.
[47] L.D. Euillades, P.A. Euillades, N.C. Riveros, M.H. Masiokas, L. Ruiz, P. Pitte, S. Elefante, F. Casu, S. Balbarani, Detection of glaciers displacement time-series using SAR, Remote Sens. Environ. 184 (2016) 188–198.
[48] A. Pepe, Generation of Earth's surface three-dimensional (3-D) displacement time-series by multiple-platform SAR data, in: Time Series Analysis and Applications, IntechOpen, 2017.
[49] S. Samsonov, N. d'Oreye, Multidimensional time-series analysis of ground deformation from multiple InSAR data sets applied to Virunga Volcanic Province, Geophys. J. Int. 191 (2012) 1095–1108.
[50] S. Samsonov, N. d'Oreye, B. Smets, Ground deformation associated with post-mining activity at the French–German border revealed by novel InSAR time series method, Int. J. Appl. Earth Obs. Geoinf. 23 (2013) 142–154.
[51] S.V. Samsonov, N. d'Oreye, Multidimensional small baseline subset (MSBAS) for two-dimensional deformation analysis: case study Mexico City, Can. J. Rem. Sens. 43 (2017) 318–329.
[52] S. Samsonov, Three-dimensional deformation time series of glacier motion from multiple-aperture DInSAR observation, J. Geodes. 93 (2019) 2651–2660.
[53] S. Samsonov, A. Dille, O. Dewitte, F. Kervyn, N. d'Oreye, Satellite interferometry for mapping surface deformation time series in one, two and three dimensions: a new method illustrated on a slow-moving landslide, Eng. Geol. 266 (2020), 105471.
[54] L. Guo, J. Li, Z.W. Li, L.X. Wu, X. Li, J. Hu, H.L. Li, H.Y. Li, Z.L. Miao, Z.Q. Li, The surge of the Hispar Glacier, central karakoram: SAR 3-D flow velocity time series and thickness changes, J. Geophys. Res. Solid Earth 125 (2020), e2019JB018945.
[55] F. Casu, S. Elefante, P. Imperatore, I. Zinno, M. Manunta, C. De Luca, R. Lanari, SBAS-DInSAR parallel processing for deformation time-series computation, IEEE J. Sel. Top. Appl. Earth Obs. Rem. Sens. 7 (2014) 3285–3296.
[56] C. De Luca, I. Zinno, M. Manunta, R. Lanari, F. Casu, Large areas surface deformation analysis through a cloud computing P-SBAS approach for massive processing of DInSAR time series, Remote Sens. Environ. 202 (2017) 3–17.
[57] S.-H. Hong, S. Wdowinski, S.-W. Kim, J.-S. Won, Multi-temporal monitoring of wetland water levels in the Florida Everglades using interferometric synthetic aperture radar (InSAR), Remote Sens. Environ. 114 (2010) 2436–2447.
[58] D. Lin, L. Guoxiang, Z. Rui, W. Xiaowen, Y. Bing, T. Jia, Z. Heng, A multi-platform MC-SBAS method for extracting long-term ground deformation, Acta Geod. Cartogr. Sinica 45 (2016) 213.
[59] L. Bai, L. Jiang, H. Wang, Q. Sun, Spatiotemporal characterization of land subsidence and uplift (2009–2010) over wuhan in central China revealed by terrasar-X insar analysis, Rem. Sens. 8 (2016) 350.
[60] Q. Zhao, H. Lin, L. Jiang, F. Chen, S. Cheng, A study of ground deformation in the Guangzhou urban area with persistent scatterer interferometry, Sensors 9 (2009) 503–518.
[61] C.-S. Yang, Q. Zhang, C.-Y. Zhao, Q.-L. Wang, L.-Y. Ji, Monitoring land subsidence and fault deformation using the small baseline subset InSAR technique: a case study in the Datong Basin, China, J. Geodyn. 75 (2014) 34–40.
[62] M. Peng, C. Zhao, Q. Zhang, Z. Lu, Z. Li, Research on spatiotemporal land deformation (2012–2018) over Xi'an, China, with multi-sensor SAR datasets, Rem. Sens. 11 (2019) 664.
[63] C. Beibei, G. Huili, L. Xiaojuan, L. Kunchao, W. Yanbing, W. Pengfei, Relationship between load density and land subsidence in typical groundwater funnel area of Beijing, China, J. Basic Sci. Eng. 21 (2013) 1046–1056.
[64] Y. Morishita, Nationwide urban ground deformation monitoring in Japan using Sentinel-1 LiCSAR products and LiCSBAS, Prog. Earth Planet. Sci. 8 (2021) 1–23.
[65] D.L. Galloway, T.J. Burbey, Regional land subsidence accompanying groundwater extraction, Hydrogeol. J. 19 (2011) 1459–1486.
[66] C. Zhou, H. Gong, B. Chen, M. Gao, Q. Cao, J. Cao, L. Duan, J. Zuo, M. Shi, Land subsidence response to different land use types and water resource utilization in Beijing-Tianjin-Hebei, China, Rem. Sens. 12 (2020) 457.
[67] E. Chaussard, P. Milillo, R. Bürgmann, D. Perissin, E.J. Fielding, B. Baker, Remote sensing of ground deformation for monitoring groundwater management practices: application to the Santa Clara Valley during the 2012–2015 California drought, J. Geophys. Res. Solid Earth 122 (2017) 8566–8582.
[68] S.W. Park, S.H. Hong, Nonlinear modeling of subsidence from a decade of InSAR time series, Geophys. Res. Lett. 48 (2021), e2020GL090970.
[69] Y. Du, G. Feng, L. Liu, H. Fu, X. Peng, D. Wen, Understanding land subsidence along the coastal areas of Guangdong, China, by analyzing multi-track MTInSAR data, Rem. Sens. 12 (2020) 299.
[70] H. Zhao, H. Qian, Y. Li, J.-B. Peng, Land subsidence model under dual effects of groundwater pumping and construction loading, J. Earth Sci. Environ. 1 (2008).
[71] J. Baek, S.-W. Kim, H.-J. Park, H.-S. Jung, K.-D. Kim, J.W. Kim, Analysis of ground subsidence in coal mining area using SAR interferometry, Geosci. J. 12 (2008) 277–284.
[72] Z.W. Li, Z.F. Yang, J.J. Zhu, J. Hu, Y.J. Wang, P.X. Li, G.L. Chen, Retrieving three-dimensional displacement fields of mining areas from a single InSAR pair, J. Geodes. 89 (2015) 17–32.
[73] Z. Yang, Z. Li, J. Zhu, G. Feng, Q. Wang, J. Hu, C. Wang, Deriving time-series three-dimensional displacements of mining areas from a single-geometry InSAR dataset, J. Geodes. 92 (2018) 529–544.
[74] X. Rao, Y. Tang, Small baseline subsets approach of DInSAR for investigating land surface deformation along the high-speed railway, in: Proceedings of the Land Surface Remote Sensing II, 2014, p. 92601C.
[75] S. Salvi, S. Stramondo, G. Funning, A. Ferretti, F. Sarti, A. Mouratidis, The Sentinel-1 mission for the improvement of the scientific understanding and the operational monitoring of the seismic cycle, Remote Sens. Environ. 120 (2012) 164–174.
[76] J. Biggs, T. Wright, Z. Lu, B. Parsons, Multi-interferogram method for measuring interseismic deformation: Denali Fault, Alaska, Geophys. J. Int. 170 (2007) 1165–1179.
[77] H. Wang, T. Wright, Satellite geodetic imaging reveals internal deformation of western Tibet, Geophys. Res. Lett. 39 (2012).
[78] J.R. Elliott, J. Biggs, B. Parsons, T. Wright, InSAR slip rate determination on the Altyn Tagh Fault, northern Tibet, in the presence of topographically correlated atmospheric delays, Geophys. Res. Lett. 35 (2008).
[79] O. Cavalié, C. Lasserre, M.-P. Doin, G. Peltzer, J. Sun, X. Xu, Z.-K. Shen, Measurement of interseismic strain across the Haiyuan fault (Gansu, China), by InSAR, Earth Planet Sci. Lett. 275 (2008) 246–257.
[80] R. Jolivet, C. Lasserre, M.P. Doin, S. Guillaso, G. Peltzer, R. Dailu, J. Sun, Z.K. Shen, X. Xu, Shallow creep on the Haiyuan fault (Gansu, China) revealed by SAR interferometry, J. Geophys. Res. Solid Earth 117 (2012).
[81] E. Hussain, A. Hooper, T.J. Wright, R.J. Walters, D.P. Bekaert, Interseismic strain accumulation across the central North Anatolian Fault from iteratively unwrapped InSAR measurements, J. Geophys. Res. Solid Earth 121 (2016) 9000–9019.
[82] Z. Li, E.J. Fielding, P. Cross, Integration of InSAR time-series analysis and water-vapor correction for mapping postseismic motion after the 2003 Bam (Iran) earthquake, IEEE Trans. Geosci. Rem. Sens. 47 (2009) 3220–3230.
[83] K. Wang, Y. Fialko, Observations and modeling of coseismic and postseismic deformation due to the 2015 Mw 7.8 Gorkha (Nepal) earthquake, J. Geophys. Res. Solid Earth 123 (2018) 761–779.
[84] Y. Wen, Z. Li, C. Xu, I. Ryder, R. Bürgmann, Postseismic motion after the 2001 Mw 7.8 Kokoxili earthquake in Tibet observed by InSAR time series, J. Geophys. Res. Solid Earth 117 (2012).
[85] C. Yang, T. Wang, S. Zhu, B. Han, J. Dong, C. Zhao, Co-seismic inversion and post-seismic deformation mechanism analysis of 2019 California earthquake, Rem. Sens. 13 (2021) 608.
[86] C. Zhao, Z. Lu, Q. Zhang, J. de La Fuente, Large-area landslide detection and monitoring with ALOS/PALSAR imagery data over Northern California and Southern Oregon, USA, Remote Sens. Environ. 124 (2012) 348–359.
[87] A. Novellino, F. Cigna, A. Sowter, M.F. Syafiudin, D. Di Martire, M. Ramondini, D. Calcaterra, Intermittent small baseline subset (ISBAS) InSAR analysis to monitor landslides in Costa Della Gaveta, Southern Italy, in: Proceedings of the 2015 IEEE International Geoscience and Remote Sensing Symposium, IGARSS, 2015, pp. 3536–3539.
[88] R.-F. Chen, C.-Y. Lee, H.-Y. Yin, H.-Y. Huang, K.-P. Cheng, C.-W. Lin, Monitoring the deep-seated landslides by using ALOS/PALSAR satellite imagery in the disaster area of 2009 Typhoon Morakot, Taiwan, in: Proceedings of the Workshop on World Landslide Forum, 2017, pp. 239–247.

[89] L. Sun, J.-P. Muller, J. Chen, Time series analysis of very slow landslides in the three Gorges region through small baseline SAR offset tracking, Rem. Sens. 9 (2017) 1314.
[90] Z.-W. Li, Investigation of the seasonal oscillation of the permafrost over Qinghai-Tibet Plateau with SBAS-InSAR algorithm, Diqiu Wuli Xuebao 56 (2013) 1476–1486.
[91] R. Zhao, in: Z. Li (Ed.), Permafrost Deformation Model Establishment and Active Layer Thickness Inversion Based on SBAS-InSAR, Central South University, 2014.
[92] L. Liu, T. Zhang, J. Wahr, InSAR measurements of surface deformation over permafrost on the North Slope of Alaska, J. Geophys. Res.: Earth Surf. 115 (2010).
[93] F. Chen, H. Lin, Z. Li, Q. Chen, J. Zhou, Interaction between permafrost and infrastructure along the Qinghai–Tibet Railway detected via jointly analysis of C-and L-band small baseline SAR interferometry, Remote Sens. Environ. 123 (2012) 532–540.
[94] R. Zhao, Z.-W. Li, G.-c. Feng, Q.-j. Wang, J. Hu, Monitoring surface deformation over permafrost with an improved SBAS-InSAR algorithm: with emphasis on climatic factors modeling, Remote Sens. Environ. 184 (2016) 276–287.
[95] Z. Jianjun, L. Zhiwei, H. Jun, Research progress and methods of InSAR for deformation monitoring, Acta Geod. Cartogr. Sinica 46 (2017) 1717.
[96] Z. Jianjun, Y. Zefa, L. Zhiwei, Recent progress in retrieving and predicting mining-induced 3D displace-ments using InSAR, Acta Geod. Cartogr. Sinica 48 (2019) 135.
[97] J. Hu, Z. Li, X. Ding, J. Zhu, L. Zhang, Q. Sun, Resolving three-dimensional surface displacements from InSAR measurements: a review, Earth Sci. Rev. 133 (2014) 1–17.
[98] A. Manconi, F. Casu, Joint analysis of displacement time series retrieved from SAR phase and amplitude: impact on the estimation of volcanic source parameters, Geophys. Res. Lett. 39 (2012).
[99] R. Zhao, in: F. Yang, G. Zhang (Eds.), Research on Model and Method of Geometric Calibration for Space-Borne SAR, Liaoning Technical University, 2017.
[100] R. Michel, J.P. Avouac, J. Taboury, Measuring ground displacements from SAR amplitude images: application to the Landers earthquake, Geophys. Res. Lett. 26 (1999) 875–878.
[101] N.B. Bechor, H.A. Zebker, Measuring two-dimensional movements using a single InSAR pair, Geophys. Res. Lett. 33 (2006).
[102] J.D. Moore, H. Yu, C.-H. Tang, T. Wang, S. Barbot, D. Peng, S. Masuti, J. Dauwels, Y.-J. Hsu, V. Lambert, Imaging the distribution of transient viscosity after the 2016 Mw 7.1 Kumamoto earthquake, Science 356 (2017) 163–167.
[103] R. Jolivet, P.S. Agram, N.Y. Lin, M. Simons, M.P. Doin, G. Peltzer, Z. Li, Improving InSAR geodesy using global atmospheric models, J. Geophys. Res. Solid Earth 119 (2014) 2324–2341.
[104] J. Catalão, G. Nico, R. Hanssen, C. Catita, Merging GPS and atmospherically corrected InSAR data to map 3-D terrain displacement velocity, IEEE Trans. Geosci. Rem. Sens. 49 (2011) 2354–2360.
[105] D. Bekaert, A. Hooper, T. Wright, A spatially variable power law tropospheric correction technique for InSAR data, J. Geophys. Res. Solid Earth 120 (2015) 1345–1356.

Shaowei Li was born in Hunan, China, in 1997. He is currently pursuing the M.S. degree in surveying and mapping with the Department of Surveying and Remote Sensing, School of Geosciences and Info-Physics. His research interests include InSAR data processing, monitoring the inter-seismic deformation and modelling

Wenbin Xu received the Ph.D. degree in Geophysics from King Abdullah University of Science and Technology, Saudi Arabia in 2015. He was a postdoc researcher with the Berkeley Earthquake Laboratory, University of California, Berkeley and an assistant professor with the Department of Land Surveying and Geo-Informatics, the Hong Kong Polytechnic University, Kowloon, Hong Kong. He is a Professor and leads the Lab of Volcano and Earthquake Research in the School of Geoscience and Info-Physics, Central South University, Changsha, China. His research primarily focuses on the use of space geodesy to study ground deformation associated with a variety of geophysical and anthropogenic processes.

Zhiwei Li received the Ph.D. degree in geodesy and surveying engineering from Central South University, Hunan, China, in 2005. He is a Professor at the School of Geosciences and Info-Physics, Central South University of China. His main research interests include modeling and mitigating the atmospheric delays for InSAR, mining subsidence monitoring and parameter estimation, permafrost parameters inversion by InSAR. His research has been supported by several projects of the National Natural Science Foundation of china